

## A Layer-Based Mesh Generator and Scheme for 3D Printing Simulation

Ming-Hsiao Lee<sup>1,\*</sup>, Shou-I Chen<sup>2</sup>, Wen-Hwa Chen<sup>3</sup> and Ying Mao<sup>3</sup>

**Abstract:** 3D Printing, also called Additive Manufacturing, has become a promising manufacturing method to produce parts in various fields as it can produce parts even with very irregular shapes in a relatively shorter process and time. However, during the printing process, some problems could decrease the accuracy and quality of the printed parts, such as warpage due to thermal strains, deformation due to inadequate supports, etc. The finite element method is most commonly adopted to evaluate engineering problems in advance to reduce possible failures; however, the element meshes, needed for analyses, are always irregularly distributed, especially for irregular objects, and cannot match the layer-by-layer growing shapes of the printed parts in the 3D printing process. Without a proper element mesh, the analysis cannot be performed. To overcome this problem, a layer-based mesh generator combined with a corresponding scheme for the 3D Printing simulation is proposed and developed. With the proposed methods, the analysis models can be designed and generated to match the growing shapes, i.e., layer-by-layer, and used to simulate the layer-by-layer growing behavior in the 3D printing process. Moreover, the proposed schemes directly adopt the Stereo-Lithography (STL) formatted geometric data as the geometry model on which the mesh generation and simulation are based. This makes them even easier to use since the STL geometry format is a De facto standard format used in the 3D printing industry. Several simulation cases have been conducted to demonstrate the effectiveness and efficiency of these proposed schemes.

**Keywords:** 3D printing, mesh generator, layer-by-layer, layer-based.

### 1 Introduction

3D printing has become a popular method to produce parts in various fields because of its promising features, e.g., it can produce complicated parts with irregular shapes more easily than traditional manufacturing methods. However, during implementing 3D printing to manufacture parts, some issues will rise and decrease the accuracy and quality of the printed parts, such as warpage due to thermal strains, collapse due to inadequate supports, etc. In order to overcome those problems and reduce the manufacturing failures,

---

<sup>1</sup> National Center for High-performance Computing, NARL, Hsinchu 30013, Taiwan.

<sup>2</sup> China University of Technology, Taipei, Taiwan.

<sup>3</sup> National Tsing Hua University, Hsinchu 30013, Taiwan.

\* Corresponding Author: Ming-Hsiao Lee. Email: mhlee@nchc.narl.org.tw.

it is advised to evaluate the processes in advance to obtain information for tackling possible defects. The numerical simulation is one of the efficient ways to evaluate engineering problems.

For simulating the 3D printing process, there are various approaches. Some research takes the macro-scale approach and some take the micro-scale approach. In the micro-scale approach, as the metal 3D printing uses metal powder to produce parts, the behavior of the melting and sintering processes significantly affects the properties of the final parts. Many studies have worked on this topic [Kolossof, Boillant, Glardon et al. (2004); Li, Li, Qi et al. (2014); Loh, Chua, Yeong et al. (2015); Megahed, Mindt, NDri et al. (2016)]. In the macro-scale approach, the usual way to simulate the behaviors of the 3D printing process is to analyze the part, as a whole, subjected to thermal strains. In this way, the analysis has not taken into account the layer-by-layer growing characteristic of 3D printing. Therefore, when the simulation just considers the model as a whole, the results are proved to be wrong as shown in Fig. 1.

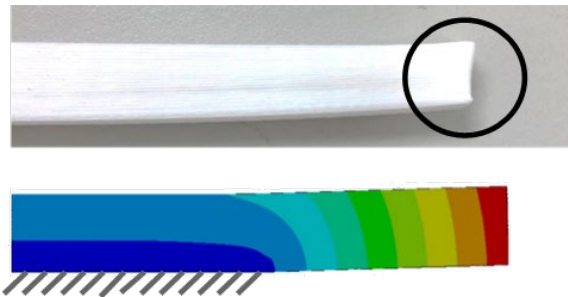


**Figure 1:** Simulation taking the model as a whole generates wrong results

The main reason is that the material is paved layer by layer. Once a layer is paved, before the next layer is deposited, it deforms due to the thermal strains caused by the cooling of temperature. Then, the next layer will be paved on the top of the already-deformed layers. Thus, each layer of material is not deformed at the same time, and it cannot be analyzed as a whole to obtain the deformation results. In order to simulate the additively-growing situation, the simulation should adopt a layer-by-layer mechanism. As the 3D printing simulation is still a new field, especially the layer-by-layer analysis, there still are not many solutions to successfully obtain accurate results. Zeng et al. [Zeng, Kai, Pal et al. (2015)] proposed an equivalent model to speed up thermal analysis for the 3D printing simulation. Liu et al. [Liu, Sparks and Liou (2015)], Li et al. [Li, Liu and Guo (2016)], and Michaleris [Michaleris (2014)] started from small-scale models which were regular and easy for mesh generation to simulate the local thermal and structural behaviors of the metal 3D printing. When the small and local models are used, the mapped meshing technique can be adopted to generate layer-arranged element meshes for layer-by-layer analyses. However, this may not work for complicated-shaped models. Keller et al. [Keller, Neugebauer and Ploshikhin (2013); Keller and Ploshikhin (2014)] proposed a method which extracts residual strains from a small-scale model and then applies the residual strains to a large-scale model, which can be irregular, for a layer-by-layer

analysis. It has proved to be an effective way for simulating 3D printing processes. In those studies, the three-dimensional layer-based meshes were generated on the basis of the CAD and sliced data. Livesu et al. [Livesu, Cabiddu and Attene (2018)] also used sliced geometric data to generate the mesh for the 3D printing simulation. In that, in order to generate layer-based mesh, sliced data needs to be created first. However, the most common adopted Geometric data in the 3D printing industry is STL formatted data. This work proposes a layer-based mesh generation method directly based on the STL formatted data so that the mesh generation and simulation process will be more efficient and straight-forward for the 3D printing simulation.

In order to do the layer-by-layer simulation, the analysis model also must follow the same condition, i.e., each layer is horizontally paved. However, it is hard to generate a layer-based mesh model with commonly-used finite element packages. The finite element meshes, normally generated by free-mesh generator, are always irregularly distributed for parts with irregular shapes as shown in Fig. 2(a). This type of meshes cannot match the required horizontally-arranged condition as shown in Fig. 2(b) and cannot be used to do a layer-by-layer simulation.

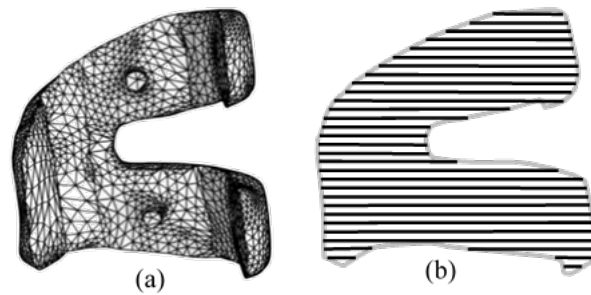


**Figure 2:** Mesh by free-meshing (a) cannot match layer-by-layer configuration (b)

Even though the mapped meshing method, which can generate meshes with brick elements, is adopted, for irregular parts, the meshes still cannot match the layer-by-layer requirement, as shown in Fig. 3.

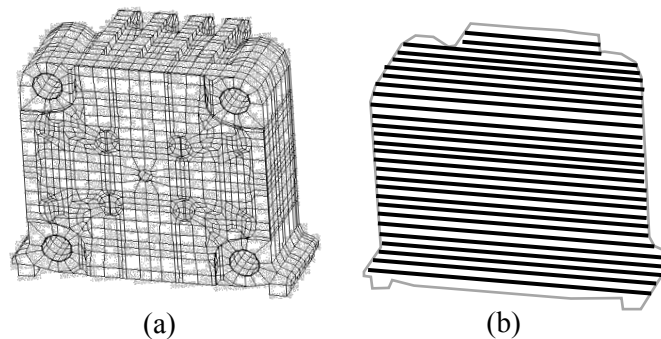


**Figure 3:** Mesh by mapped-meshing (a) cannot match layer-by-layer configuration (b)

Thus, in order to overcome above problems, a layer-based mesh generator combined with a corresponding scheme for the 3D Printing Simulation is proposed. It includes a layer-based auto-mesh generator by which the analysis models, element meshes, are generated on the layer basis, i.e., arranged and organized layer by layer so that each layer's elements can be turned active or inactive to simulate the material deposition behavior. In this proposed scheme, the loading is the temperature difference as that in the printing process instead of residual stains proposed by Keller et al. [Keller and Ploshikhin (2014)]. Moreover, these proposed schemes also directly adopt the STL geometry data which is more commonly-used and convenient in the 3D printing field. In addition, the layer-based mesh generator and analysis scheme is automatically processed without any manual operation. This advantage makes the proposed method efficient and easy to use.

## **2 Method**

As mentioned above, if the simulation considers the model as a whole, the results are proved to be wrong. In order to simulate the additively-growing situation, the simulation should be performed in a layer-by-layer way. To implement that, a layer-based mesh is needed. However, the traditional methods used to generate meshes for an irregular shaped object, either free-meshing or mapped meshing, cannot generate an element mesh matching the layer-by-layer arrangement. Here proposed is a new auto-mesh generator based on layers. With that, a layer-by-layer simulation process can be adopted to simulate the 3D printing processes. Moreover, this layer-based mesh generator directly uses the STL geometry to produce meshes.

### ***2.1 Geometry in STL format***

STL geometry, i.e., geometry in STL format, is different from traditional CAD geometry, which uses many types of lines, surfaces, volumes to represent the geometry model. On the contrary, the STL geometry uses only triangular facets to form the faces of objects to represent the object's geometry. Compared with complicated geometric entities used in CAD systems, e.g., Bezier surfaces, Non-Uniform Rational Basis Spline (NURBS), etc. STL geometry adopts only one type of geometric entity, the triangular facet. Due to that, the STL geometry may be not as accurate as other sophisticated geometric entities; however, due to its simplicity, it is very flexible to represent irregular-shaped geometry, often encountered in computer graphics and 3D printing. Hence, it is popularly adopted in the 3D printing industry. Currently, in the 3D printing industry, Geometry data in STL format has been considered a De facto standard format to transfer geometry data between different systems, e.g., CAD systems and 3D printers. Due to this, the proposed schemes adopt STL geometry as the geometry model for simulation, i.e., the analysis model is generated based on it. This STL-based way can simplify the geometry data transfer and handling. Consequently, this can make the simulation process easier and faster.

### ***2.2 Automatic layer-based mesh generator***

Once the geometry data is ready, a layer-based element mesh can be generated in the following procedure, as shown in Fig. 4,

- (1) Import the geometry data in STL format, Fig. 4(a)
- (2) Pave points layer by layer over the entire analysis domain, Fig. 4(b)
- (3) Delete those points outside the analysis domain and keep the points inside the domain, Fig. 4(c). The mechanism to judge if a point is inside or outside the analysis domain is shown in Fig. 5, where a reference point outside the domain is first defined. Connect the reference point and the discussed point to form a line and then check how many times the line crosses the boundary. If the number of times is odd, e.g., line 1 crosses boundary once, the point is inside the domain, otherwise it is outside the domain, e.g., line 2 crosses twice.
- (4) Convert all points, as the center of elements, in the same layer to cubic elements, and link them together. Repeat the same operation for each layer, then the layer-based element mesh can be obtained, as shown in Fig. 4(d).

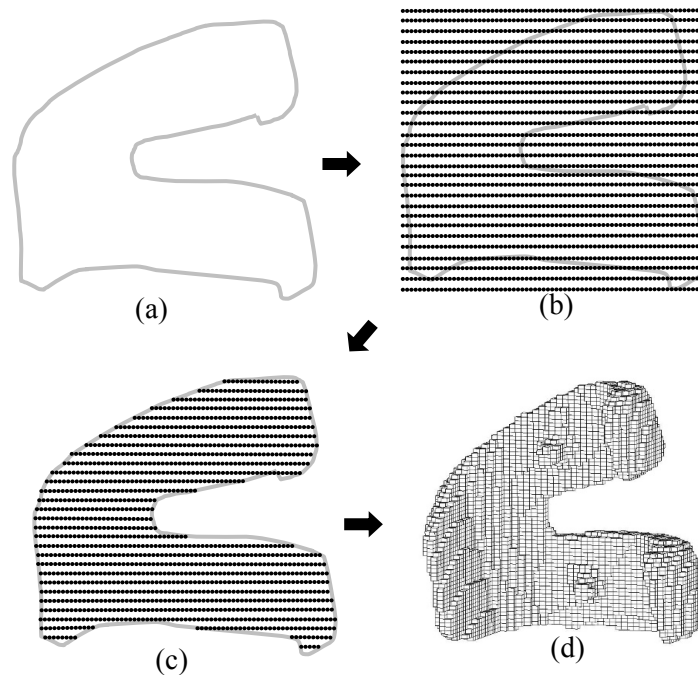


**Figure 4:** Layer-based mesh generation

Since the element mesh is arranged on the layer basis, the mesh model can meet the layer-by-layer analysis process easily. Namely, after the layer-based element mesh is ready, a layer-by-layer analysis procedure can be performed with it directly. Moreover, since the layer-by-layer points are so regular arranged that this process can be performed automatically by a program, part of the proposed schemes.

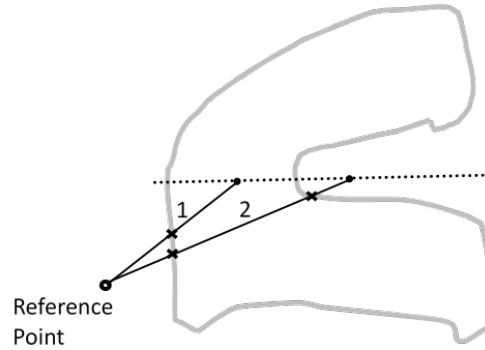


**Figure 5:** Mechanism to check if a point is inside the domain

### 2.3 Layer-by-layer simulation procedure

After the layer-based element mesh is ready, a layer-by-layer analysis procedure can be performed with it. In the beginning, all the element layers are deactivated first, and then activated layer by layer in order, i.e., in each analysis step. Activating a layer (of mesh) is just like newly-paved material layer in the real printing process. The layer-by-layer analysis procedure is as follows:

- (1) Get the layer-based mesh ready
- (2) Deactivated all element layers
- (3) Activate one layer, labeled 1 as shown in Fig. 6(a)
- (4) Apply a temperature drop to the newly-activated layer, i.e., a thermal loading
- (5) Perform a structural analysis step (using ANSYS or ABAQUS solver), in which the temperature is cooled down to room temperature 25°C, to obtain the displacements and stresses due to thermal shrinkage. The deformation is like that shown in Fig. 6(b), where dashed lines denote the original shape.
- (6) Activate the next element layers, labeled 2 as shown in Fig. 6(c). Since the previous layer is deformed, the newly paved layer is no longer regular like layer 1. This matches the real printing.
- (7) Repeat (4)~(6) to do next analysis step and activate next layer.

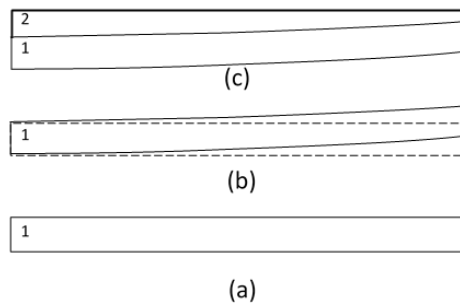


**Figure 6:** Layer by layer simulation process

Since the number of real printing layers is rather large, to simplify and speed up the analysis, each analysis layer can include several real material layers. This can reduce significant computing time and get acceptable results.

### 3 Results and discussion

To validate the proposed schemes, a long bar case was investigated. The size of the long bar is  $100\text{ mm} \times 20\text{ mm} \times 10\text{ mm}$ , as shown in Fig. 7. It was printed with a Fused Deposition Modeling (FDM) 3D printer. The material used was Polylactic Acid (PLA). About the material properties of PLA, the Young's modulus is 3600 MPa, Poisson's ratio is 0.35, the thermal expansion coefficient is  $8.5 \times 10^{-5}\text{ mm/mm}^\circ\text{C}$  and the melting temperature is  $165^\circ\text{C}$ . To conduct this case, the long bar was partially fixed on the bottom to the working table, i.e.,  $\frac{3}{4}$  of the bottom is fixed and another  $\frac{1}{4}$  is free of constraint. This is to simulate the common failure in which end portion of a long part detaches from the working table due to the thermal stains induced during the printing process. After detachment occurs, the printing continues and the part deforms visibly. To simulate this situation can let us know the relationship between the thermal strains and deformation, and the behavior of the layer-by-layer printing. To observe how it deformed during the printing process, the temperature was cooled down to room temperature  $25^\circ\text{C}$ . The experimental printed parts and final deformed shapes are shown in Fig. 7. There were more than 10 printed specimens. The maximum displacements of those specimens in Z direction range from 2.8~4.1 mm as shown in Fig. 8. This is because the line-by-line and layer-by-layer printing is a long process and the printing results could be affected by tiny environmental differences in different printings. As shown in Figs. 7(b), 7(d) and 7(e), the free end of the bar was deformed due to the thermal strains caused by cooling situation.

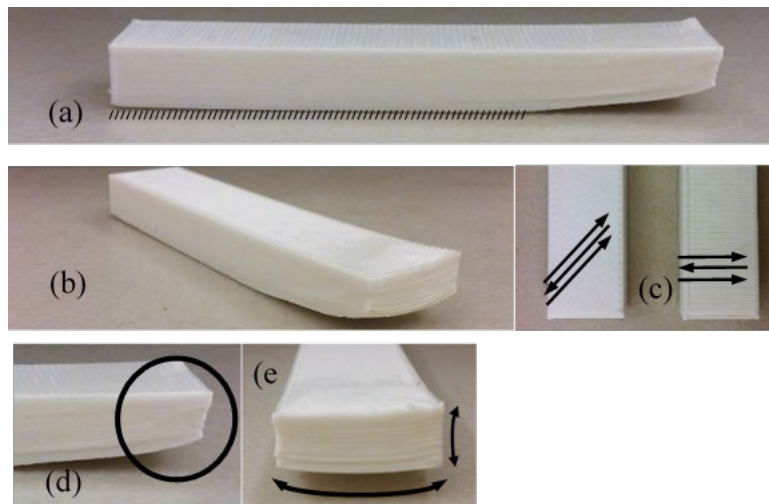


Figure 7: Printed results



**Figure 8:** Printed results (10 pieces)

The bar is bent at the longitudinal end as shown in Fig. 7(a). In addition, the layer-by-layer effect can be observed at the end edge as shown in Fig. 7(d), i.e., the lower layers deformed before the upper layers were deposited and the end edge is no longer straight. This phenomenon also applies in the lateral direction as shown in Fig. 7(e). The results show that the thermal strain will cause the bar to bend in both longitudinal and lateral direction and the layer-by-layer effect causes a complicated deformation phenomenon.

Another phenomenon that can also be observed is that the printing hatching orientation does not have an obvious effect on the deformation results in these prints. It is because the printing machine, used here, changes hatching orientation by  $90^\circ$  in each consecutive layer so that the thermal strains can be considered isotropic on average. Two different initial orientation printing parts as shown in Fig. 7(c) produce similar results. Therefore, when the hatching orientation changes regularly in each layer, the thermal strains can be considered isotropic.

To simulate this case, the proposed schemes were adopted. The boundary constraint was set to be the same as the real printing, 3/4 partially fixed. The only loading was the temperature dropping from the melting temperature  $165^\circ\text{C}$  to room temperature  $25^\circ\text{C}$ . The melting temperature is chosen because it is assumed that the material is stress free above melting temperature. The analysis was conducted layer by layer. The results are shown in Fig. 9. The maximum displacement is 3.14 mm at the very end of the bar. The displacement results are close to those of the experimental printings as shown in Tab. 1. Moreover, the deformed shape is also consistent with those of the experimental prints. This validates the effectiveness of the proposed schemes.

**Table 1:** Maximum displacement comparison between experiments and analysis

	<b>Experiments (mm)</b>	<b>Analysis (mm)</b>
Maximum displacement	2.8~4.1	3.14

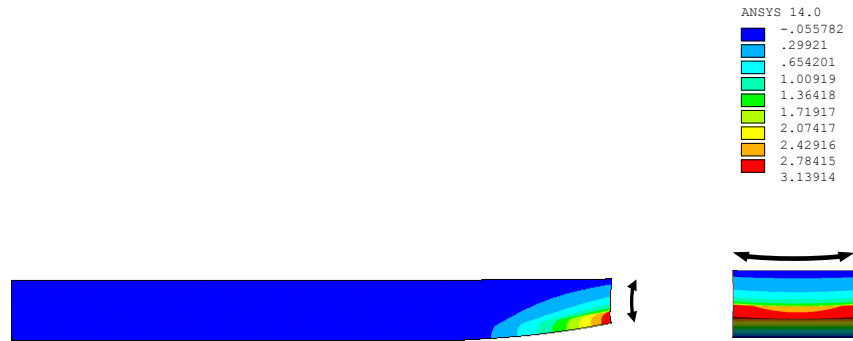


**Figure 9:** Simulation results: deformation and displacements (mm)

After the validation, the proposed scheme was adopted to simulate two more complicated cases to further demonstrate the capability of the proposed schemes.

The second case is about a metal 3D printing. In metal 3D printing, since the thermal strains are much larger, the deformation could be more serious. This situation could not only decrease the size accuracy of the printed parts but also damage the powder paving blade during printing. Moreover, due to the residual stresses, the shapes before and after the supports are removed could be apparently different. It means a significant inaccuracy could rise and the size accuracy is more difficult to reach. Therefore, evaluation in advance becomes more important. Here a metal 3D printing simulation was conducted. The size and shape of the specimen is shown in Fig. 10(a). This is a typical test part with supports.

The material used is titanium, and its Young’s modulus is 120 GPa, Poisson’s ratio is 0.3, thermal expansion coefficient is  $8.2 \times 10^{-6}$  mm/mm °C and melting temperature is 1650°C. To simulate this case, the specimen with supports is fixed to the base plate and the supports are removed after the printing is finished. During the printing process, the temperature of material is cooling down. At the end, the temperature of the whole model is cooled down to room temperature 25°C. The simulation results are shown in Fig. 10. It is found that the specimen deforms dramatically after the supports are removed as shown in Fig. 10(e). The maximum displacement at the end of the cantilever is 3.3 mm. In addition to the main deformation, some local deformations also exist during the printing, as shown in Fig. 10(d). Fig. 10(f) shows a real printing, after cut from the base. The maximum displacement is 2.6 mm. Although there is still a gap between the simulation and experiment as shown in Tab. 2, the trend of the printing has been captured.

**Table 2:** Maximum displacement comparison (metal 3D printing)

	Experiment (mm)	Analysis (mm)
Maximum displacement	2.6	3.3

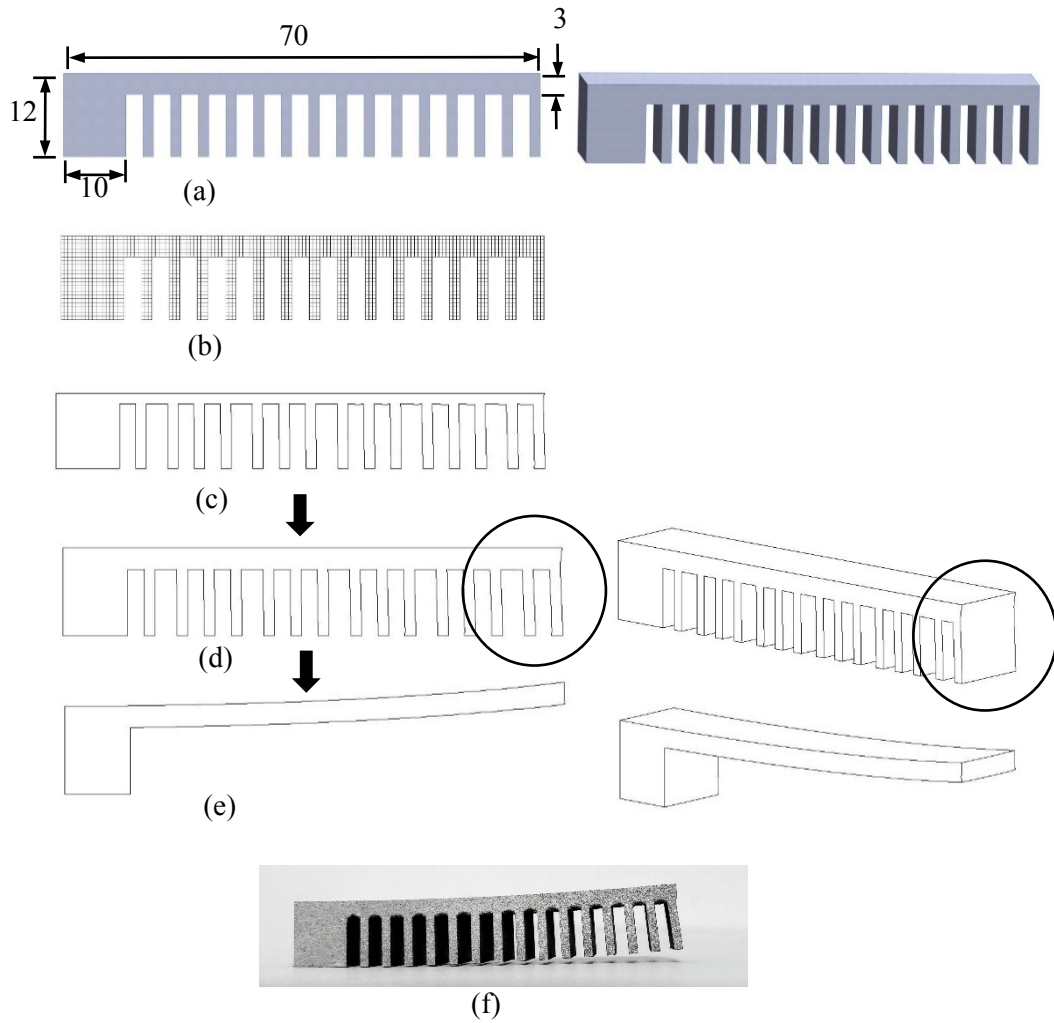


**Figure 10:** Metal 3D printing: (a)-(e) simulation, (f) printed part after cutting from base

One of the main advantages of 3D printing is its flexibility to print complicated parts with irregular shapes; however, it is difficult to generate a layer-by-layer mesh for them with traditional methods as mentioned above. Without a proper mesh, the simulation cannot proceed. After the proposed approach, the layer-by-layer simulation, has been validated via previous cases, in order to demonstrate that the proposed layer-based mesh generator can also handle complicated parts, a highly irregular object was adopted. The object of the third case is a medical implant, an artificial joint as shown in Fig. 11(a). Since the shapes of medical implants usually are very irregular, it becomes more difficult to generate layer-based meshes for 3D printing simulation. Here, the proposed auto-mesh generator can generate a layer-based element mesh as shown in Fig. 11(b). Once the element mesh is available, the simulation in a layer-by-layer way as described above can be performed. The results are shown in Fig. 11(c). The growing shapes during the

printing are also shown. The maximum displacement is 3.8 mm. This case demonstrates the capability of the proposed layer-based mesh generator and layer-by-layer simulation scheme. It can handle objects with very complicated irregular shapes.

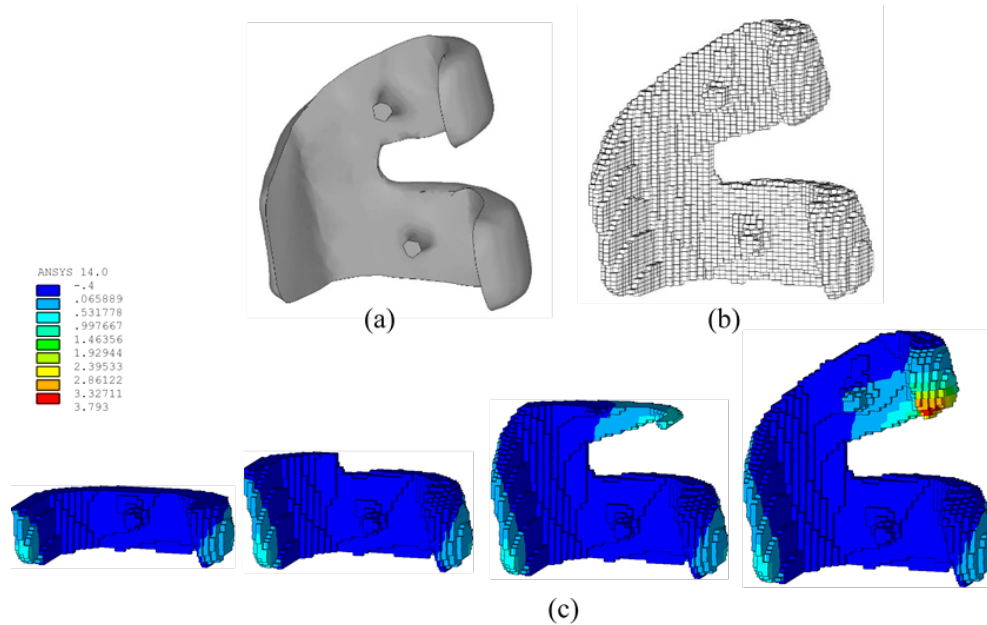


**Figure 11:** Layer-by layer simulation of irregular object

#### 4 Conclusions

3D Printing has already shown its promising advantage for manufacturing. To take full advantage of it, the shortcomings of it need to be avoided. For that, the numerical simulation can be a good way to reduce the failures. However, the 3D printing process includes so many complicated phenomena that it has become a great challenge to researchers and engineers. Even just the additively-growing phenomena of the printing process is much more complicated than and different from other traditional engineering cases. This work has proposed a new layer-based mesh generator combined with a layer-by-layer analysis scheme which can roughly catch the behavior of the printing process. With this, the printing results can be predicted in advance. The information could also be useful for improving the printing results. However, there still are many details to explore to further improve the effectiveness and accuracy of the simulations.

**Acknowledgement:** The authors would like to thank the Ministry of Science and Technology of Taiwan for financially supporting this research under Contract MOST-107-2221-E-492-015.

**References**

- Keller, N.; Neugebauer, F; Ploshikhin, V.** (2013): Thermo-mechanical simulation of additive layer manufacturing of titanium aerospace structure. *LightMAT*.
- Keller, N.; Ploshikhin, V.** (2014): New Method for fast predictions of residual stress and distortion of AM parts. *Solid Freeform Fabrication Symposium*, vol. 25.
- Kolossov, S.; Boillat, E.; Glardon, R.; Fischer, P.; Locher, M.** (2004): 3D FE simulation for temperature evolution in the selective laser sintering process. *International Journal of Machine Tools & Manufacture*, vol. 44, pp. 117-123.
- Li, C.; Liu, J. F.; Guo, Y. B.** (2016): Prediction of residual stress and part distortion in selective laser melting. *3rd CIRP Conference on Surface Integrity*, vol. 45, pp. 171-174.
- Li, H.; Li, H.; Qi, L.; Luo, J.; Zuo, H.** (2014): Simulation on deposition and solidification processes of 7075 Al alloy droplets in 3D printing technology. *Transactions of Nonferrous Metals Society of China*, vol. 24, pp. 1836-1843.
- Liu, H.; Sparks, T.; Liou, F.** (2015): Residual stress and deformation modeling for metal additive manufacturing processes. *Proceedings of the World Congress on Mechanical, Chemical, and Material Engineering*.
- Livesu, M.; Cabiddu, D.; Attene, M.** (2018): slice2mesh: meshing sliced data for the simulation of AM Processes. *Smart Tools and Applications in Graphics*.
- Loh, L.; Chua, C.; Yeong, W.; Song, J.; Mapar, M. et al.** (2015): Investigation and an effective modelling on the Selective Laser Melting (SLM) process with aluminum alloy 6061. *International Journal of Heat and Mas Transfer*, vol. 80, pp. 288-300.
- Megahed, M.; Mindt, H.; NDri, N.; Duan, H.; Desmaison, O.** (2016): Metal additive-manufacturing process and residual stress modeling. *Integrating Materials and Manufacturing Innovation*, vol. 5, no. 1.
- Michaleris, P.** (2014); Modeling metal deposition in heat transfer analyses of additive manufacturing processes. *Finite Elements in Analysis and Design*, vol. 86, pp. 51-60.
- Zeng, K.; Pal, D.; Teng, C.; Stucker, B. E.** (2015): Evaluation of effective thermal conductivity of support structures in selective laser melting. *Additive Manufacturing*, vol. 6, pp. 67-73.